

# **CHAPTER 2 LITERATURE REVIEW ON LIQUEFACTION AND GROUND DENSIFICATION FOR LIQUEFACTION MITIGATION**

## **2.1 Liquefaction–Induced Failure Mechanisms**

One of the most dramatic causes of damage of structures during earthquakes has been the development of liquefaction in saturated cohesionless deposits. These deposits have tendency to densify when subjected to earthquake loading. However, when saturated, the tendency to densify causes the excess pore water pressure to increase. This, in turn, results in the effective stress of soil to decrease. As a consequence, the cohesionless deposit will lose a substantial strength and a subsequent reduction in soil volume until the excess pore water pressure has a chance to dissipate. The phenomenon of pore pressure build-up following with the loss of soil strength is known as liquefaction (Committee on Earthquake Engineering, 1985).

The potential damage caused by liquefaction phenomena includes: 1) Loss of bearing capacity, 2) Excessive settlement, 3) Lateral spreading, 4) Flow failure, and 5) Ground oscillation. The following sections will discuss each phenomenon.

### **2.1.1 Loss of Bearing Capacity**

The softening of soil causes the soil to lose strength. This, in turn, causes the loss of support of foundations of structures. This weakening process results in bearing failure as shown on Figure 2.1.

### **2.1.2 Excessive Settlement**

This phenomenon usually accompanies the loss of bearing capacity of the liquefied soil. The structure above the liquefied soil (shown in cross-hatched zone) tilts and settles

excessively. Conversely, buried structures, such as tanks and pipelines, may float upward through the liquefied soil as shown on Figure 2.1.

### **2.1.3 Lateral Spreading**

Lateral spreading involves large horizontal displacement on the ground surface as a result of liquefaction in a shallow underlying soil deposit. It generally occurs on the surface with gentle slopes range from 0.3 to 3 degrees (Committee on Earthquake Engineering, 1985). In large-magnitude earthquakes, lateral spreading causes tremendous damage, often times disruptive and pervasive though rarely catastrophic. Figure 2.2 shows the mechanism of lateral spreading. The top figure shows the initial condition and the bottom one shows the condition after liquefaction occurs (shown in cross-hatched zone). Note that the surface layer breaks into blocks bounded with fissures while moving down a gentle slope. These blocks may settle and tilt with respect to each other.

### **2.1.4 Flow Failure**

According to the Committee on Earthquake Engineering (1985), flow failure is the most catastrophic failure caused by liquefaction, mostly developed in coastal area. It involves movement of large soil masses traveling tens of kilometers on slopes greater than 3 degrees. The failure is even worse under water. Figure 2.3 shows diagram of flow failure. The top figure shows the condition prior to liquefaction and the bottom one shows the condition after liquefaction. Note that liquefaction develops beneath the ground surface causing the soil to flow downward a steep slope and finally rests after traveling many kilometers.

### **2.1.5 Ground Oscillation**

Ground oscillation occurs on a very gentle slope when lateral spreading does not occur. Liquefaction (shown in cross-hatched zone) results in overlying blocks of soil on the ground surface as shown on Figure 2.4. The soil blocks bounded by fissures oscillate back and forth on top of an underlying liquefied zone. Figure 2.4 shows this phenomenon with the top and bottom figures illustrate conditions before and after liquefaction occurs, respectively.

### 2.1.6 Pore Pressure Generation

As it is understood from the definition of liquefaction, pore pressure generation plays an important role. The magnitude of pore pressure can be estimated in terms of excess pore pressure ratio ( $r_u$ ). The value of  $r_u$  can be estimated by using data from laboratory tests (De Alba, et al., 1975; Seed, et al., 1975; Tokimatsu and Yoshimi, 1983; Marcuson, et al., 1990). Here, the excess pore water pressure ratio ( $r_u$ ) is defined as the ratio between excess pore water pressure and the initial effective vertical stress. The excess pore water pressure is defined as the difference between the total pore water pressure after being shaken and the hydrostatic pore water pressure. De Alba, et al. (1975) proposed the following equation to estimate the value of  $r_u$  for stress-controlled cyclic tests with uniform loading:

$$r_u = \frac{1}{2} + \frac{1}{\pi} \sin^{-1} \left[ 2 \left( \frac{N}{N_L} \right)^{1/\alpha} - 1 \right] \quad (2.1)$$

where:

$N_L$  = the number of cycles required to produce initial liquefaction ( $r_u = 1.0$ )

$N$  = the number of loading cycles

$\alpha$  = a constant as a function of soil properties and test conditions

It can be seen from Figure 2.5 that the excess pore pressure ratio increases quickly in the first and last loading cycles. The dashed line shows the values of  $r_u$  for  $\alpha$  equals to 0.7 and was drawn using equation (2.1).

Tokimatsu and Yoshimi (1983) used equation (2.1) to develop a relationship between  $r_u$  and factor of safety against liquefaction ( $FS_L$ ).

$$r_u = \frac{1}{2} + \frac{1}{\pi} \sin^{-1} \left[ 2 FS_L^{1/(\alpha\beta)} - 1 \right] \quad (2.2)$$

where:

$FS_L^{1/\beta} = N/N_L$  in equation (2.1)

Note that equation (2.2) is valid only for  $FS_L$  equals to or larger than unity. Marcuson, et al. (1990) used equation (2.2) and presented it as shown on Figure 2.6.

## **2.2 Ground Densification Techniques for Liquefaction Mitigation**

Due to the damages that may be caused by liquefaction as explained in the previous section, efforts have been developed to reduce the damage effects of this phenomenon. Of particular interest are efforts to densify the liquefiable soil and to provide drainage path to accelerate pore pressure dissipation during seismic loading by inclusion of column-like structure in the ground. Vibro-compaction, vibro-replacement, vibratory probe, and aggregate piers are some examples of ground improvement techniques that fit into this category.

The following section will discuss briefly the ground densification techniques using vibro-compaction, vibro-replacement and vibro-displacement stone columns, and vibratory probe method. The next section will discuss the technique using aggregate pier foundation system.

### **2.2.1 Vibro-Compaction**

Vibro-compaction (Brown and Glenn, 1976; Brown, 1977; Saito, 1977; Lopez and Hayden, 1992), sometimes referred to as vibroflotation, uses vibrating unit in the ground, which vibrates horizontally. Figure 2.7 shows the installation equipments required for this technique, which includes the vibrator, extension tubes, and a supporting crane. The combination of the first two equipments is called vibroflot. This figure also shows the typical construction process of vibro-compaction. This process includes forming a cavity in the ground using vibrator, advancing the vibrator to the desired depth, and raising and lowering the vibrator and backfilling, both processes at the same time. Vibrations are generally close to the tip of the vibrator and are produced by rotating eccentric weights mounted on a shaft. The backfill material used for this technique is typically sand. Typical spacing is 1.5 to 3.0 meters (Broms, 1991).

### **2.2.2 Stone Columns**

Stone columns technique is similar to vibro-compaction. The difference is in the backfill that is used. Stone columns generally use gravel or crushed stone as backfill. Thus, the name of stone column. Numerous publications have been published about the use of stone columns for ground reinforcement, for example by Barksdale and Bachus (1983), Munfakh, et al. (1987), Baez and Martin (1992a, 1992b), and Lopez and Hayden (1992).

In general, stone columns can be installed in two ways: dry or wet method (Munfakh, et al., 1987; Hayward Baker, 1996). In the dry method, compressed air is used to assist the advance of the vibrator. The stone is fed by pipes directly to the nose of the vibrator (bottom feed technique) as shown on Figure 2.8. Little soil is extracted during the installation. Stone columns installed using dry method are referred to as vibro-displacement stone columns.

The wet method uses water jets and the self-weight of the vibrator to advance into the cavity. Unlike the dry method, some collapsible soils are removed to the surface by the water. The stone is fed to the annulus of the vibrator, which falls by gravity and vibrations to the cavity under the nose of the vibrator (top feed technique). Stone columns installed using wet method are referred to as vibro-replacement stone columns.

Baez and Martin (1993, 1994) suggested that the typical diameter for stone columns constructed using the wet method is between 85 cm and 105 cm and between 70 cm and 90 cm for those constructed using the dry method.

The range of grain-size of soil that is suitable for densification using vibro-compaction, vibro-replacement stone columns and vibro-displacement stone columns is shown on Figure 2.9.

### **2.2.3 Vibratory Probe Method**

The vibratory probe method uses heavy vibrator that is clamped to the upper end of a long steel probe. Unlike the previous two methods, the vibratory probe method induces vertical vibrations. The vibrator is mounted on the top of the probe and does not penetrate the ground. Typical construction process includes the advance of the probe to the desired depth and densification of the soil during extraction of the probe. Backfill material is not commonly used for this method (Russell, 2001). Typical spacing is 1 to 2 meters (Broms, 1991).

Several probe designs have evolved over time. They include terra-probe (Anderson, 1974; Brown and Glenn, 1976), double tube rod and rod with projective (Saito, 1977), vibro wing (Massarsch and Broms, 1983; Massarsch and Lindberg, 1984; Massarsch, 1991), Franki TriStar probe or Y-probe (Massarsch, 1991; Neely and Leroy, 1991; Van Impe, et al., 1994; Holeyman, 1997), and Double-Y or Flexi probe (Van Impe, et al., 1994)

## **2.3 Aggregate Pier Foundation System**

The aggregate pier foundation system was developed initially by Fox in the spring of 1984 (Lawton, et al., 1994; Fox and Cowell, 1998). Fox and Lawton (1993) then registered this system in U. S. Patent in 1993. The initial objective of the development of aggregate pier foundation system was to provide a simple, practical, and economical way to improve weak soils using a stiffer material as an alternative to overexcavation/replacement technique. Since the time of the first development, the use of aggregate pier has been extensive. It has been used since 1988 to support shallow and mats foundations (Lawton and Fox, 1994; Lawton, et al., 1994b). The use of aggregate pier of particular importance is in reducing settlement of the upper-structures (Lawton and Fox, 1994a, 1994b; Fox and Edil, 2000a, 2000b; Wissmann, et al., 2000; Gaul, 2001), increasing the bearing capacity of soil (Lawton, et al., 1994b; Fox and Edil, 2000a, 2000b), increasing the uplift capacity (Lawton, et al., 1994a, 1994b; Fox and Edil, 2000a, 2000b; Hsu, 2000), increasing the lateral stress of soil (Gaul, 2001), and withstanding seismic loading (Lawton, 1999, 2000; Lawton and Merry, 2000).

### **2.3.1 Construction Process**

The typical construction process of aggregate pier foundation system can be divided into four main stages as shown on Figure 2.10:

1. Creating a cylindrical or rectangular prismatic (linear) cavity in the soil matrix by augering or trenching (Figure 2.10a),
2. Placing aggregate (clean stone) at the bottom of cavity (Figure 2.10b),
3. Making the bottom bulb by ramming the aggregate with tamper, which has 45 degrees beveled foot (Figure 2.10b), and

4. Building the shaft with undulating layers in thin lifts (12 inches or less) consisting of well-graded aggregate, typically stone as used for highway base course material (Figure 2.10c and 2.10d).

Due to the unique construction process, aggregate pier has distinct features for seismic considerations compared to other ground densification techniques that can be divided into:

1. The ramming process pushes the aggregate into the sidewalls of the cavities. This process increases the lateral stress in soil matrix (Gaul, 2001).
2. The use of well-graded aggregate results in higher shear strength of the aggregate pier element. Fox and Cowell (1998) reported that in-situ direct shear test has been performed and showed that aggregate pier has friction angle at about 50°.
3. Many case histories have shown that aggregate pier foundation system has substantial stiffness modulus (Fox and Edil, 2000a, 2000b; Wissmann, et al., 2001b).
4. Aggregate pier may serve as drainage system depends on the gradations of the soil matrix and aggregate pier elements.

Aggregate pier has typical diameter of 24 to 36 inches for cylindrical columns or 18 to 30 inches wide for rectangles (Lawton, et al., 1994a, 1994b). Generally, it is 5 to 10 feet high to a maximum of 20 feet and is set 2 feet below grade level. The typical ratio of height and width is 2 to 3. The tamper used to ram the aggregate is of high energy and relatively high frequency unit (Lawton, et al., 1994b). The diameters of the tamper vary from 15 to 32 inches.

Several studies have been published comparing the effectiveness of aggregate pier versus other ground improvement techniques. Lawton and Fox (1994) and Lawton, et al. (1994b) compared the aggregate pier foundation system and the stone columns formed by vibro-replacement method. Their study draw conflicting conclusions as to which technique is more efficient. The distinct features of aggregate pier as mentioned previously were discussed. They argued that aggregate piers are shorter, formed in a cavity rather than by soil displacement, preserves the natural cementation and fabric of soil, and produce much stiffer elements.

Fox and Edil (2000a, 2000b) discussed the use of aggregate pier over peat and highly organic soils. They argued that the traditional vibro-replacement system encounter problem

with groundwater, poor reinforcement, and capacity limitation for construction on soft organic silts and peat. Therefore, it was suggested to use the aggregate pier to overcome these problems and to get a more economical solution.

### **2.3.2 Performance of Aggregate Pier for Seismic Considerations**

Aggregate piers have been used in a wide variety soils ranging from peat to very loose coarse-grained soil and solid waste. As noted before, liquefaction most likely occurs at site with very loose to loose cohesionless soils. Therefore, aggregate pier can be used for liquefaction mitigation.

One parameter that affects the performance of aggregate pier under seismic loading is the integrity of the pier. Svinkin and Fox (1998) tested the integrity of four aggregate piers. Pile Integrity Test (PIT) was used to observe 30 inches wide and 8 feet deep aggregate piers. PIT is a non-destructive test using a hammer to generate a low strain stress wave, which propagates down the shaft of the aggregate pier. The velocity reflection is recorded and used as a basis to determine the quality of the tested material. Svinkin and Fox (1998) found that aggregate pier can be considered as a rigid body for stress wave propagation. The basis for this conclusion was that no defects or obstacles were detected between separately aggregate thin lifts. This conclusion is important pertaining to this research and will be used in the numerical modeling as will be explained in later chapters.

Wissmann, et al. (1999) argued that the behavior of aggregate pier-supported foundation system is similar to shallow foundation but with greater bearing capacity and resistance to lateral forces. During seismic loading, the foundation of the structure is subject to inertia loads vertically and horizontally. Shallow foundation resists the downward vertical force by available shear resistance on the bearing capacity failure planes. The upward vertical force (uplift force) is resisted by the weight of soil above the foundation, the weight of the structure supported by the foundation, and the weight of the foundation itself. The lateral force is resisted through the passive resistance of the soil adjacent to the foundation and through friction between the foundation and the underlying soil. The aggregate pier foundation system works in a similar way when subjected to seismic loading. In addition to that, reinforcements can be installed in the aggregate pier to provide additional resistance against the uplift force. Figure 2.11 illustrates the mechanisms of the resistance of aggregate pier foundation system against



seismic loading. The following sections discuss each feature of the aggregate pier foundation system for seismic considerations.

### **2.3.2.1 Increase in Lateral Stress**

As noted previously, the ramming process in installation of aggregate pier increases the lateral stress in soil matrix (Gaul, 2001). Handy, et al. (1999) indicates that the increase in lateral stress of soil matrix occurs not only around the cavity perimeter but also approximately one diameter below the cavity depth before compaction is conducted with a possibility of greater deep for loose sand deposit.

White, et al. (2000) also observed the increase in lateral stress of soils due to the ramming action of aggregate pier. They used prebored pressuremeter tests to study the characteristics of stiff overconsolidated glacial till soil improved by closely spacing aggregate piers. Prebored pressuremeter tests were conducted before, during, and after installation of a group of four closely spaced aggregate piers. The tests indicated that after the first and the second piers were installed the lateral stress in the soil matrix increased and then decreased after the third and fourth piers were installed. It was deduced that the lateral stress of soil reached the passive limit. The decrease of lateral stress was suspected due to horizontal compression and soil remolding. Remolding of soil matrix causes a temporary reduction in cohesion. This phenomenon suggests that the Mohr-Coulomb failure envelope for the overconsolidated soil adjusts to that of normally consolidated soil after installation of aggregate piers.

A further study was conducted by White, et al. (2000) to observe the remolding phenomenon by carrying out borehole shear tests on a different site. The tests were performed at different depths between two aggregate piers (depth of 5.5 meters) and compared to tests carried out at depths far from zone of influence of the aggregate piers. The soil condition of this site consists of canyon outwash and lakebed deposits. The test results indicated little changes in friction angle after installation of the aggregate piers both at depths between the two aggregate piers and at depths far from zone of influence. On the contrary, the cohesion showed significant changes. It decreased up to depth of 3 meters, partially reduced at depth of 3 to 4 meters and then increased with depths. This phenomenon implies that remolding occurs up to depth of 4

meters and beyond this depth compaction occurs. Figure 2.12 shows the conceptualization of zone of remolding for this site. Lateral stress of 120 kPa was induced by ramming action of aggregate pier. This value was calculated from borehole shear tests shear strength parameters. White, et al. (2000) proposed the following equation to estimate the depth of zone of remolding between two closely spaced aggregate piers:

$$z = \frac{1}{\gamma K_p} (\sigma_{pier} - 2c\sqrt{K_p}) \quad (2.3)$$

where:

$\gamma$  = buoyant unit weight

$K_p$  = coefficient of passive earth pressure

$\sigma_{pier}$  = lateral stress induced by ramming action of aggregate pier

$c$  = cohesion

Handy (2001) proved the increase in the lateral stress through stress path analogy. Figure 2.13 shows the stress path for normally consolidated soils. The consolidation stress path is represented by path EF. The angle  $\phi'$  is the soil friction angle and the angle  $\beta'$  can be determined as

$$\beta' = \sin^{-1} \left( \frac{\sin \phi'}{2 - \sin \phi'} \right) \quad (2.4)$$

Figure 2.14 shows the stress path for overconsolidated soils where the unloading stress path is represented by path FG. Handy (2001) proposed a stress reinforcement stress path due to the ramming process as shown on Figure 2.15. The ramming process is represented by path AB and path BC shows the condition after foundation loading is applied. A simpler representation is shown on Figure 2.16. Handy (2001) suggested that the friction reversals as shown on Figure 2.16 occurs with no compaction is needed. Therefore, as a consequence excess pore pressures should be negligible.

### **2.3.2.2 Increase in Density of Soil**

The ramming action of aggregate pier using beveled tamper forces the stone to the sidewall of the excavated cavity. This process builds up the lateral stress of the adjacent soil matrix and densifies the soil matrix near the aggregate pier perimeter.

By ramming, the aggregate pier is compacted to substantial density that may preclude liquefaction of the aggregate pier elements and soil matrix. Wissmann, et al. (1999) suggested that the compaction extends to 6 inches from the cavity perimeter that is created when installing the aggregate pier. Therefore, they concluded that 50 to 70 percent of the foundation area below the aggregate pier-supported foundation system is improved as non-liquefiable material.

### **2.3.2.3 Increase in Stiffness Modulus**

Aggregate pier is constructed in thin lifts, typically 12 inches or less, by ramming action using beveled tamper. This process prestrains, prestresses and densifies the adjacent soil matrix and produce a very dense and very stiff foundation, which in turn reduce the displacement upon application of loads. The displacement occurs near the top of the aggregate pier is caused by bulging. Bulging displaces the soil matrix outward and increases the lateral stress along pier-soil matrix interface.

As noted previously, the aggregate pier elements are stiffer than the surrounding soil matrix. Fox and Cowell (1998) suggested that the stiffness ratio may range from 8 to 32. Therefore, the shear stresses induced by seismic loading will be absorbed mostly by the aggregate pier elements and be proportional to the stiffness ratio between the aggregate pier and the soil matrix.

There are abundant data on the stiffness modulus of aggregate pier. In fact, modulus load tests are conducted at most of the projects using aggregate piers (Lawton, et al., 1994; Lawton and Fox, 1994; Fox and Edil, 2000; Wissmann, et al., 2000, 2001b). Wissmann, et al. (2001b) presented data from thirty-one modulus load tests carried out on residual Piedmont soils. They found that the elastic modulus of the aggregate piers vary between 115 MPa to 270 MPa (1,200 tsf to 2,800 tsf). These values correspond to the stiffness ratio between the

aggregate piers and the soil matrix varying from 5 to 60 for Standard Penetration Test (SPT) blow counts range between 3 and 50 blows/foot.

#### **2.3.2.4 Improved Drainage**

Aggregate pier may serve as drainage path for the surrounding soil matrix. This behavior depends on the gradation of the aggregate pier elements and the soil matrix. The aggregate pier elements can have coefficient of permeability two to six order of magnitude larger than that of the soil matrix. As the earthquake loading generates pore pressure within the soil matrix, the water will flow to the aggregate pier elements.

#### **2.3.3 Case Histories**

This section discusses two case histories pertaining to the performance of aggregate pier under seismic loading. The first one is by AThirty-Two@ (2001) and the second one is by Lawton (1999, 2000) and Lawton and Merry (2000).

AThirty-Two@ (2001) reported that thirty-two structures supported by aggregate piers survived the 6.8 Richter scale Nisqually earthquake in Olympia, Washington. There was no single crack or any evidence of damage detected after the structures were observed several days after the earthquake. Some of the structures are located within or in close proximity to the areas where landslides, building damage, and liquefaction occurred.

Lawton (1999, 2000) and Lawton and Merry (2000) observed the behavior of full-size aggregate piers under simulating loading of a magnitude 7.5 Richter scale earthquake. The test was performed by applying cyclic loading (alternate pushing and pulling) to the existing bridge bent through an actuator attached to a reaction frame. This reaction frame stood on shallow foundations supporting by a group of aggregate piers as shown on Figure 2.17. The behavior of the fully instrumented aggregate piers was observed. The cyclic loading consisted of lateral, uplift and compression forces, and overturning moments applied to the bent caps.

To enable the aggregate piers sustaining the lateral and uplift forces induced by cyclic loading, a steel plate was inserted at the bottom of each cavity before placing stone at the bottom. This plate was acting as an uplift steel plate. Then vertical steel uplift bars were attached to the plate near its perimeter. The bars were extended into the footing and bonded to

the footing after the concrete was placed. It was found that after being subjected to 60 cyclic loading, the aggregate pier only moved in fractions of an inch (0.9 inch of lateral displacement and less than 0.1 inch of average vertical displacement). It was also found that when compressive force was applied to the aggregate pier, the induced stress was greatest at the top and decreased with depth. For one loading cycle, the aggregate piers carried 95% of the applied compressive load. When the uplift force was applied, the induced stresses increased with depth with the steel plate installed at the bottom of the aggregate pier had the largest induced compressive stresses. These results show that the uplift force was transmitted to the soil through the uplift plates at the bottom of the aggregate piers. In fact, after a numerical analyses were conducted, it was found that the uplift bars carried between 21 and 42 percent of the peak lateral force applied.

The footings supported by the aggregate pier were founded on the ground surface. The resistance against lateral loads was obtained through the resistance along the bottom of the footings and through the passive resistance from the uplift bars being pushed into the aggregate piers. At high loads (compression or tension), the stiffness of the aggregate piers increased with increasing force. The increase was more pronounced in compression than in uplift force. These results show that aggregate piers behave as ductile material and are able to sustain large deformations without significant damage or large permanent displacements. It was suggested that the period of the aggregate pier is higher than that of deep foundation. This character of aggregate pier allows it to dissipate more energy generated by earthquake to the substructure. Hence, the use of aggregate pier system transfers less deformation and energy to the superstructure.

The stress concentration ratio, i.e. the ratio between the induced contact stress on the aggregate pier and the induced contact stress on the soil matrix is proportional to the subgrade modulus ratio, i.e. the ratio between the subgrade modulus of aggregate pier and the subgrade modulus of soil matrix (Lawton, et al., 1994). It was found that both ratios range from 25 to 45.

Lawton (1999) proposed an estimate of pullout zone for aggregate pier induced by tensile force. Figure 2.18 shows an illustration of assumed pullout zone for single aggregate pier. It can be concluded that the uplift resistance of aggregate pier comes from the effective weight of soil within the pullout zone, the shearing resistance of soil matrix, and the weight of

the uplift bars. A procedure to estimate the uplift capacity of aggregate pier elements can be found in Hsu (2000).

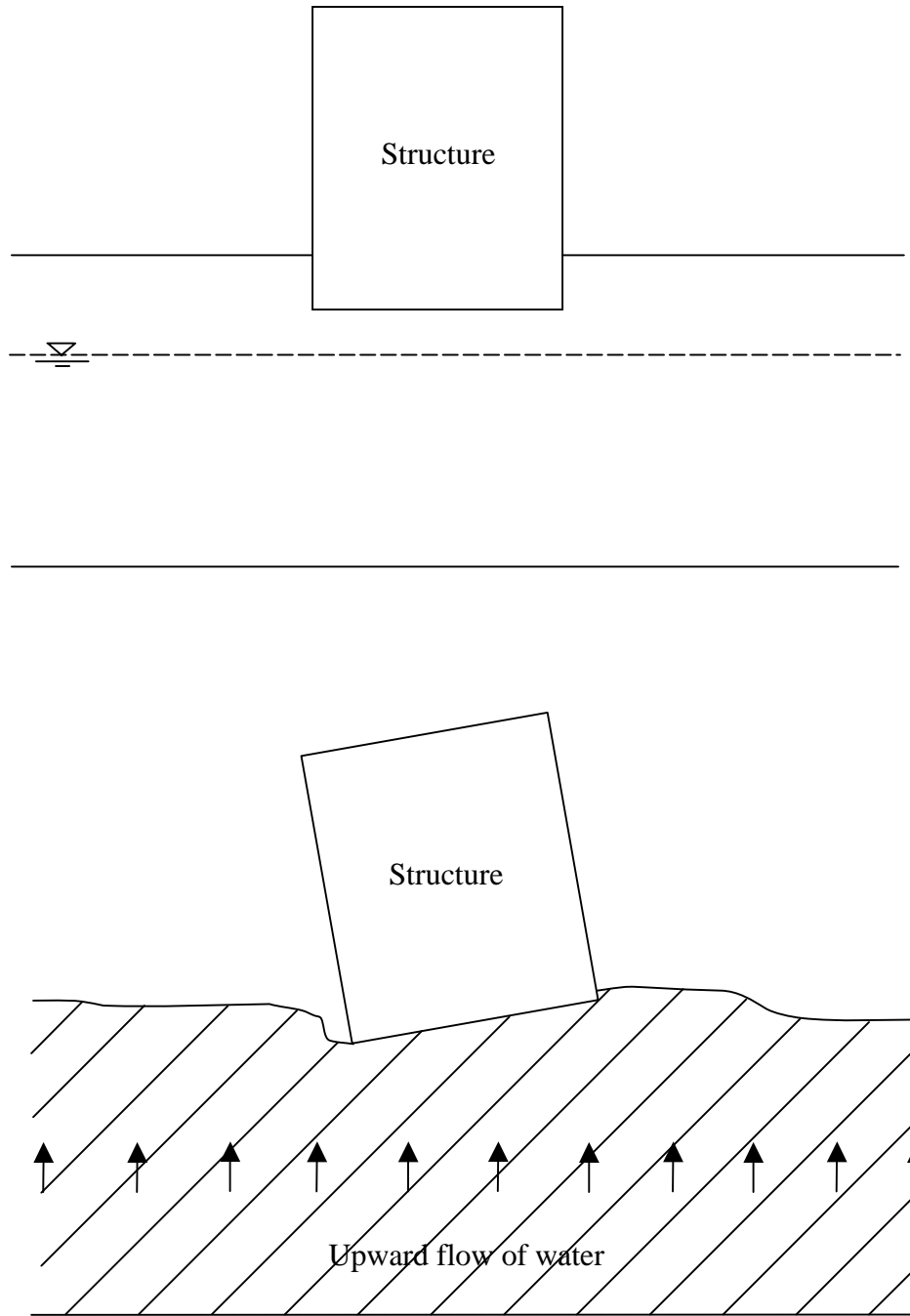


Figure 2.1 Bearing capacity failure and excessive settlement (after Youd, 1984)

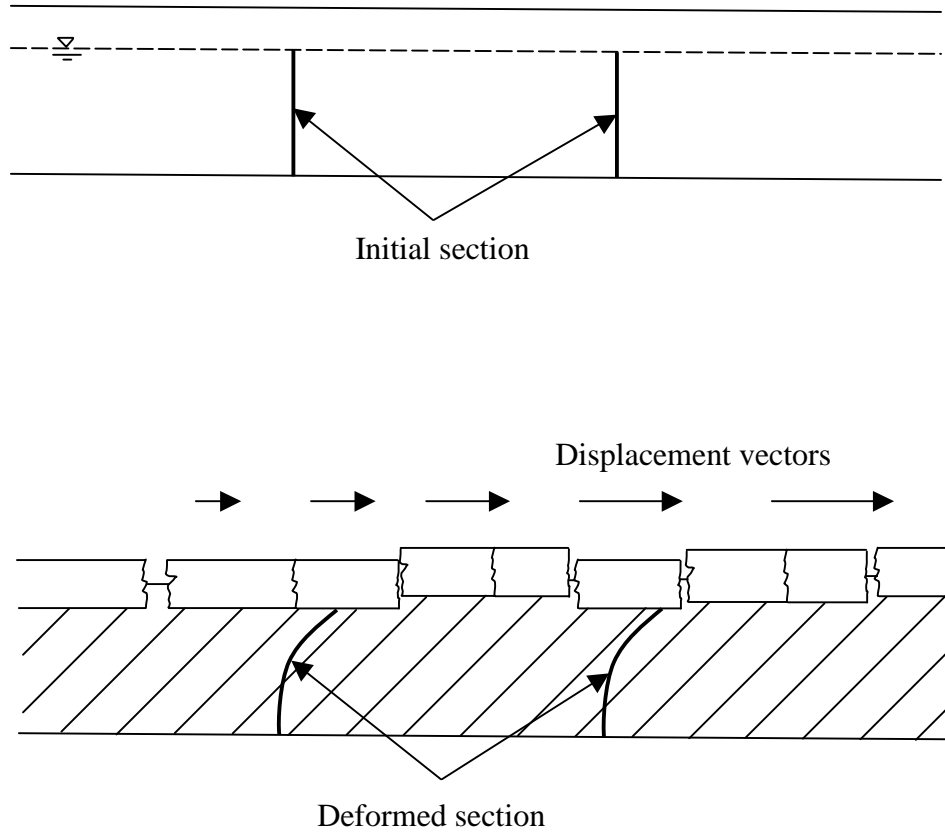


Figure 2.2 Lateral spreading (after Youd, 1984)



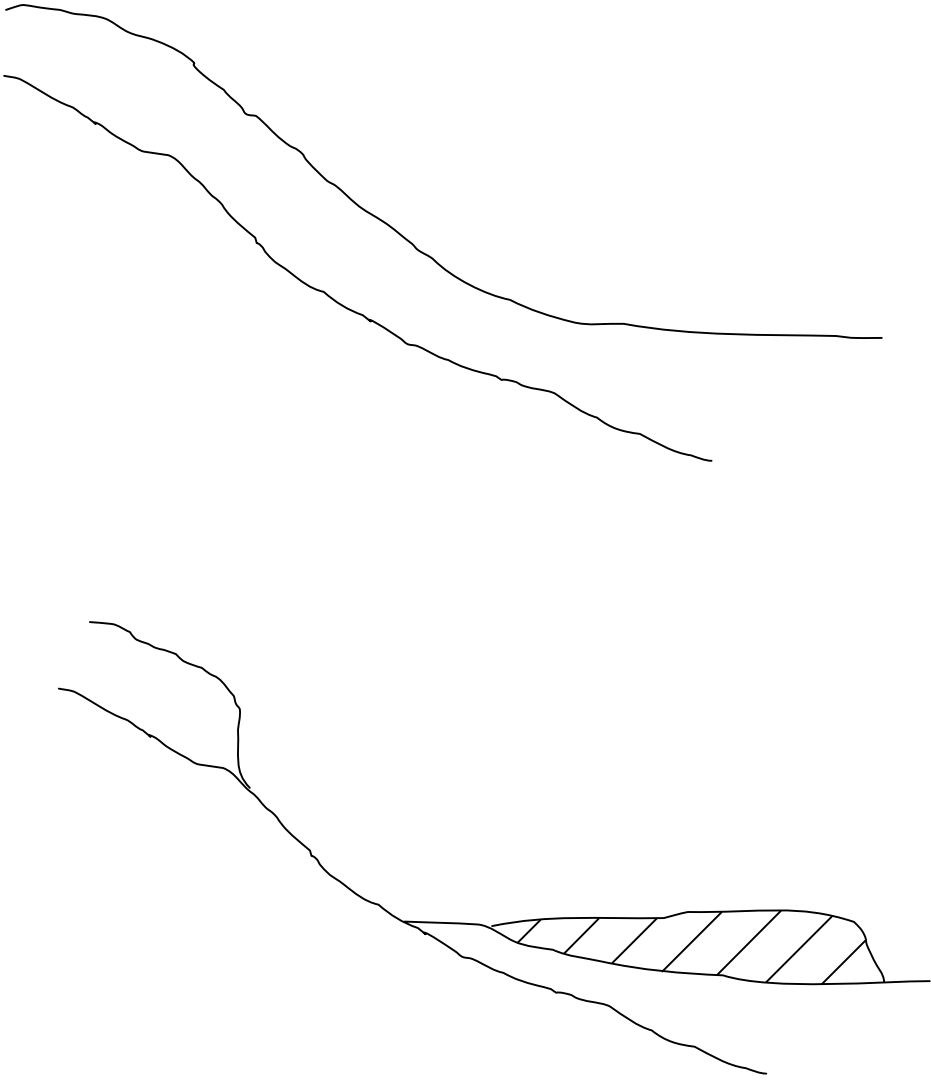


Figure 2.3 Flow failure (after Youd, 1984)

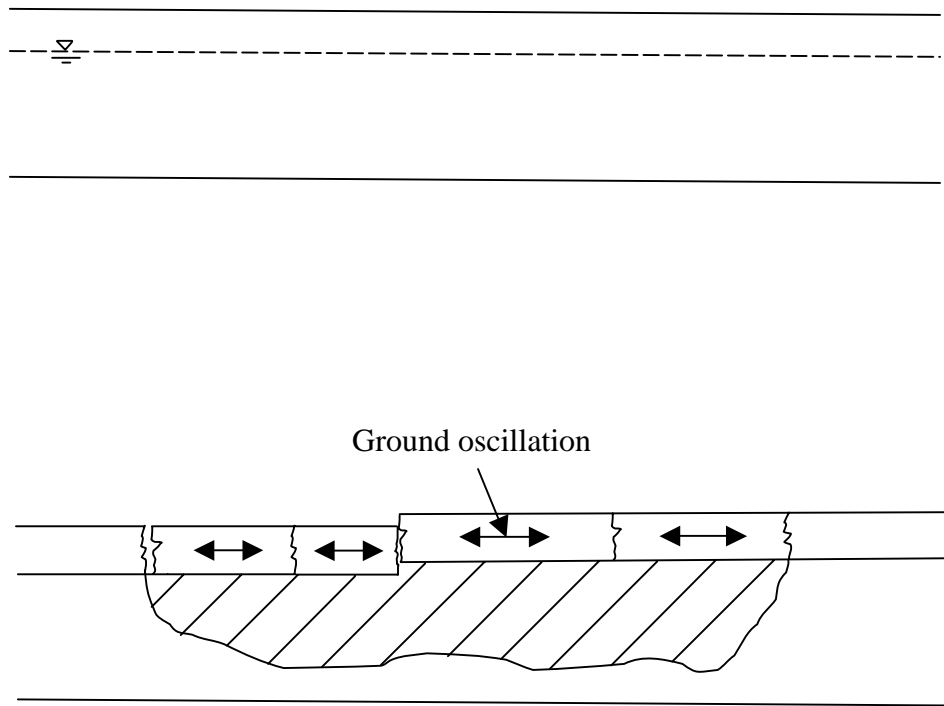


Figure 2.4 Ground oscillation (after Youd, 1984)

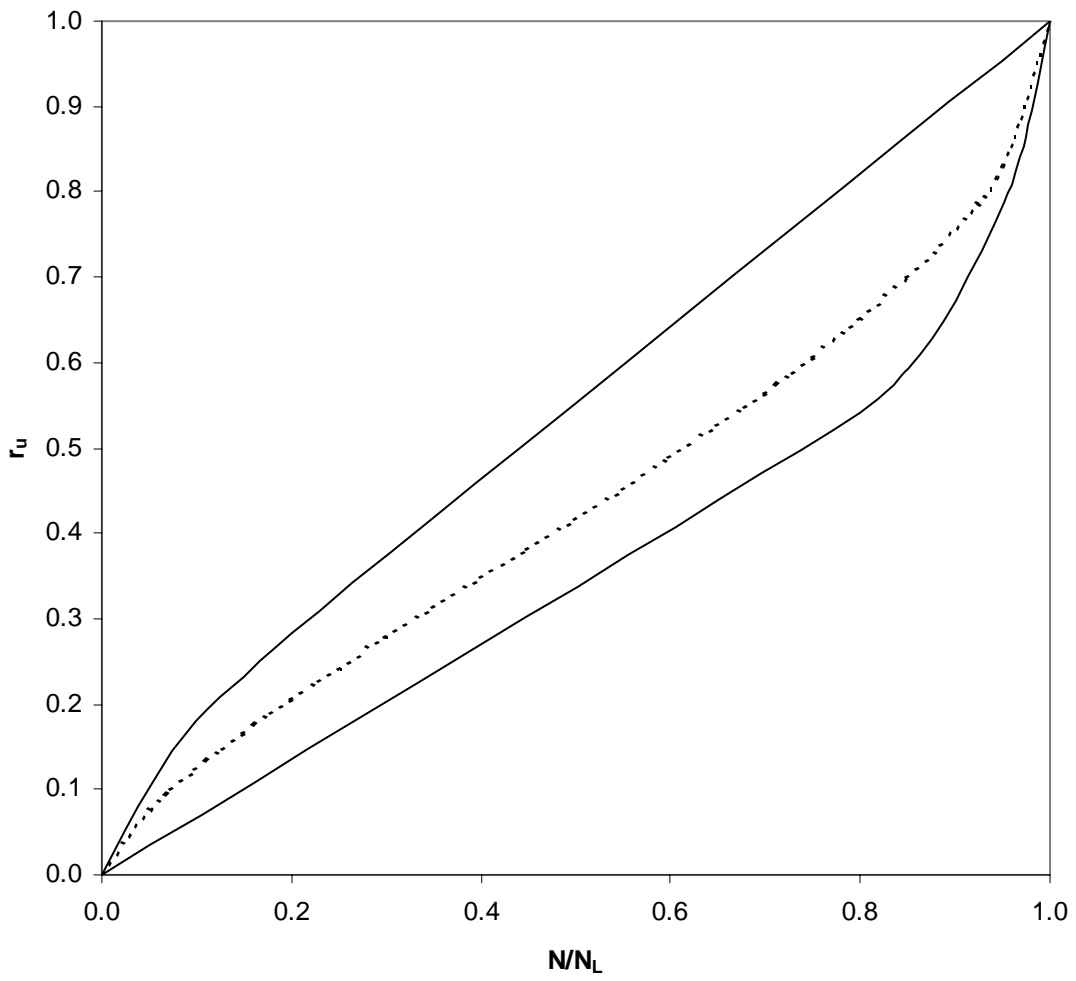


Figure 2.5 Rate of pore pressure generation in cyclic simple shear tests (after De Alba, et al., 1975)

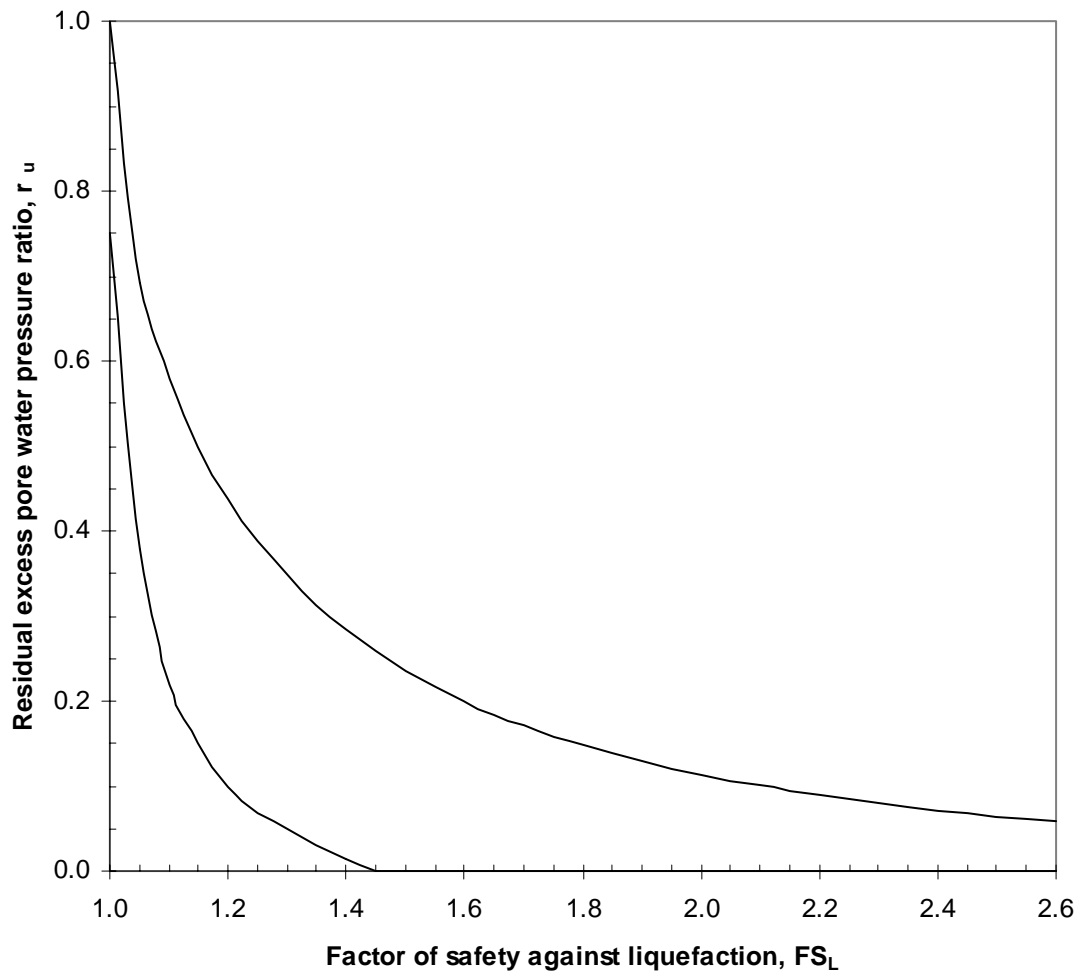


Figure 2.6 Relationship between pore pressure ratio ( $r_u$ ) and factor of safety against liquefaction ( $FS_L$ ) for sand from laboratory data (after Marcuson, et al., 1990)

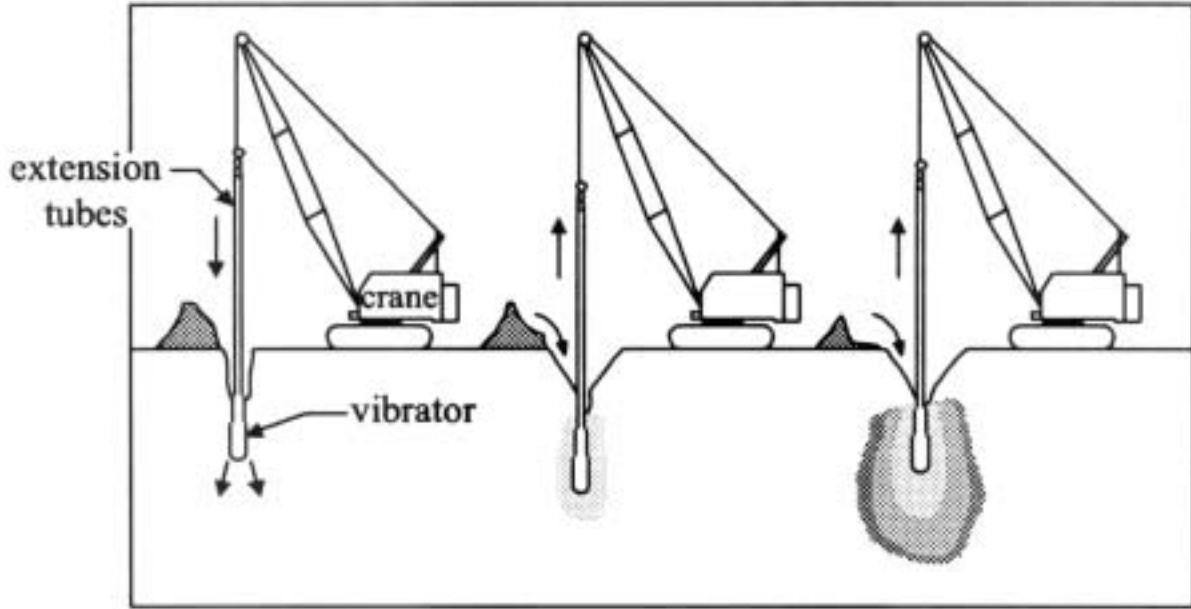


Figure 2.7 Typical construction process for vibro-compaction (Green, 2001)

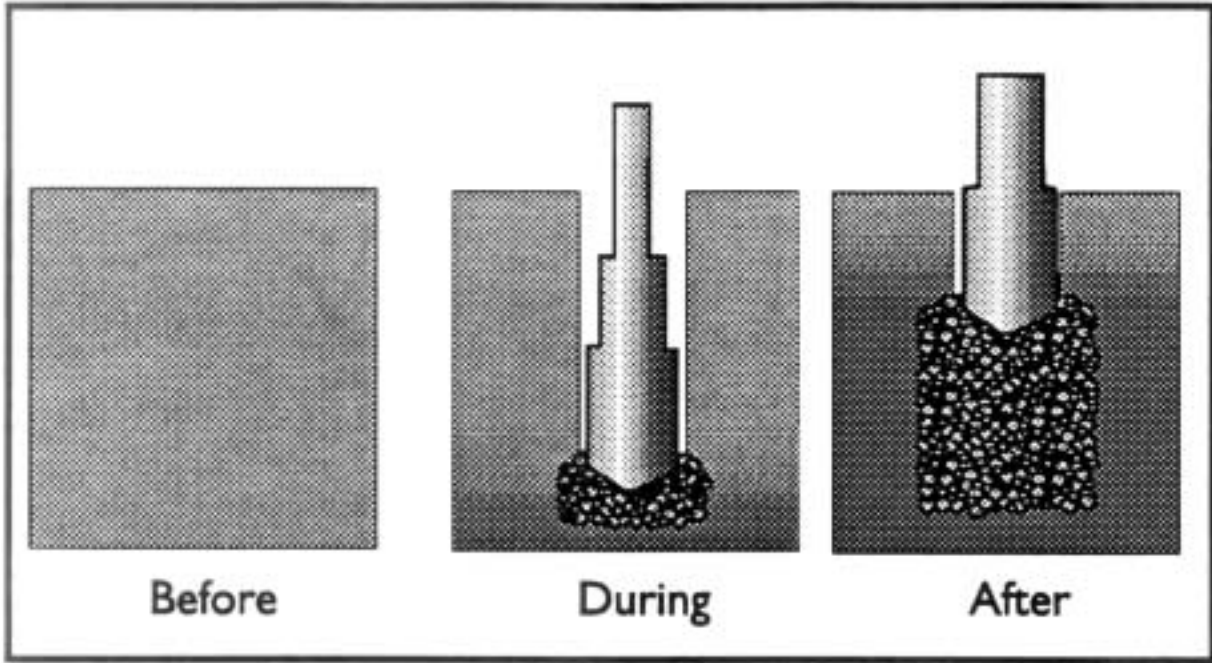


Figure 2.8 Installation of stone column using dry method: before, during, and after installation (Hayward Baker, 1996)

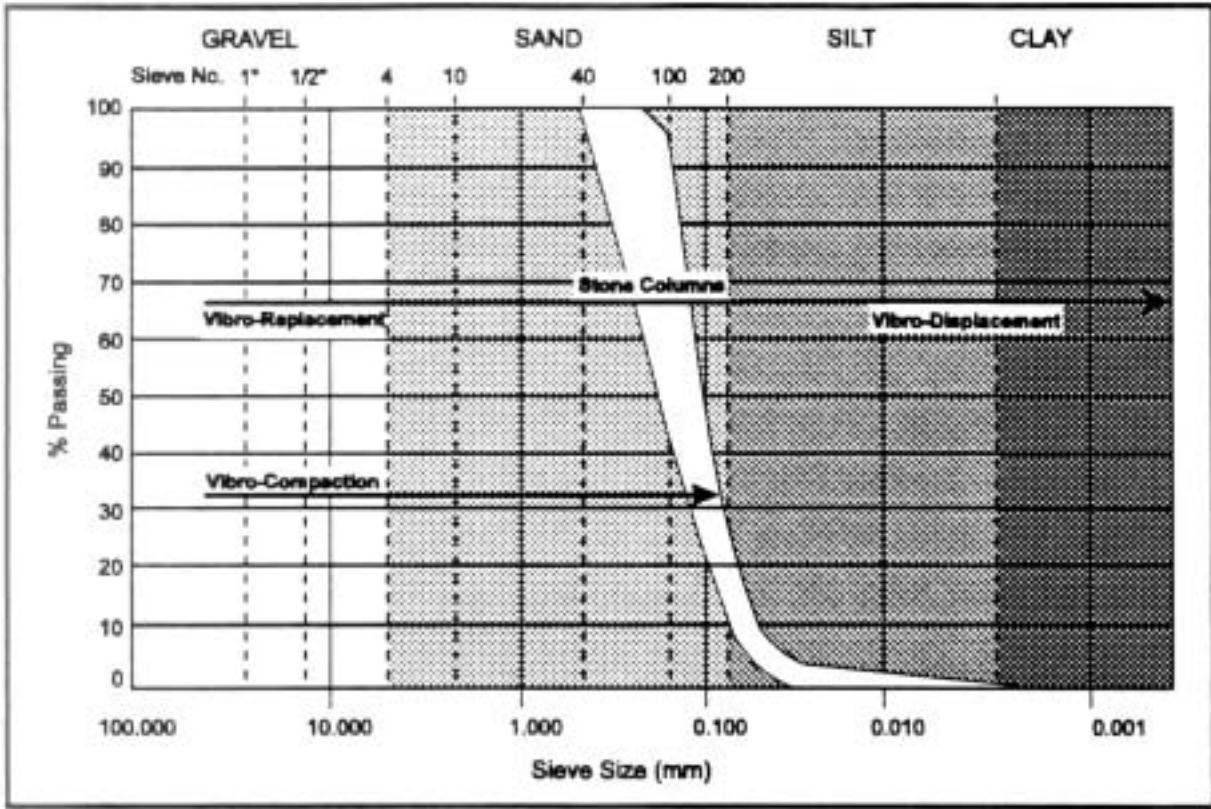


Figure 2.9 Range of grain size of soil suitable for vibro-compaction technique and stone columns (Hayward Baker, 1996)

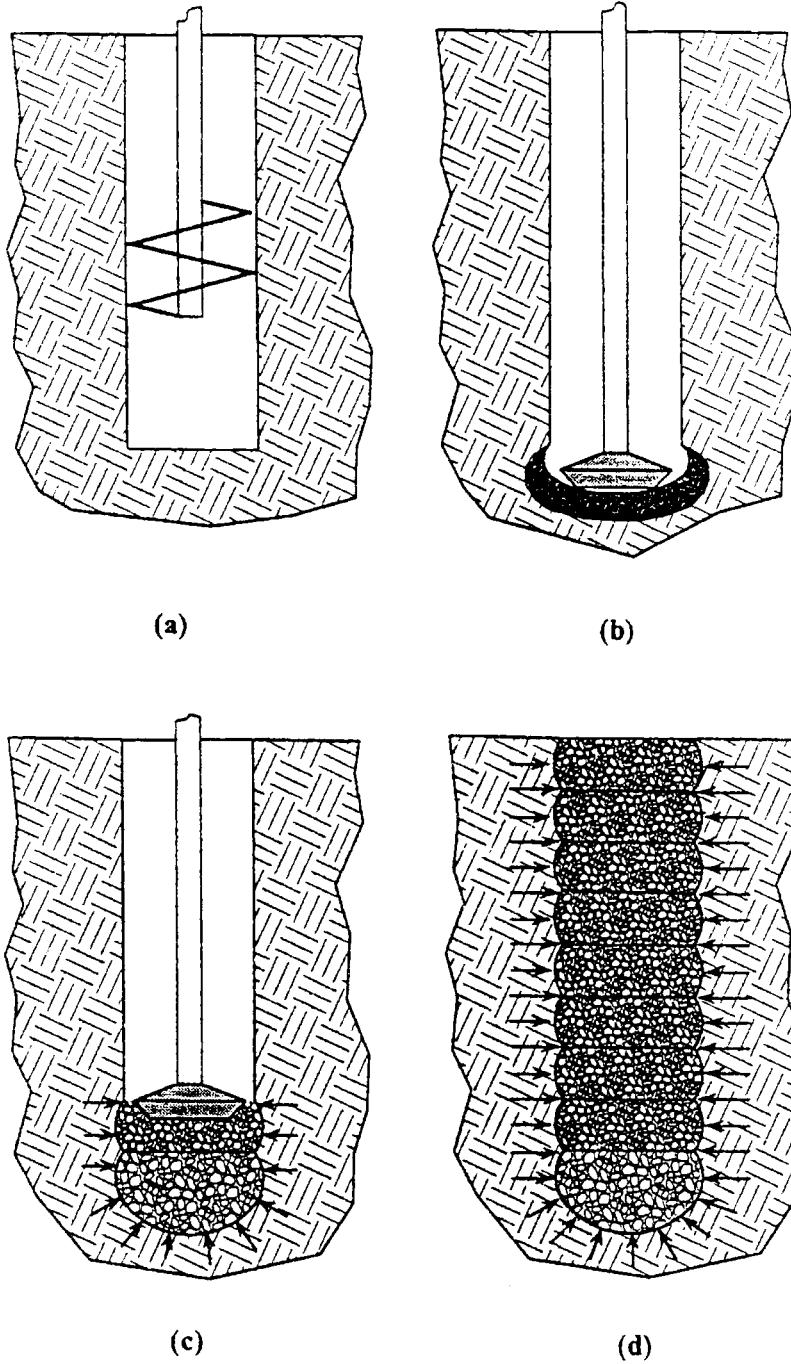


Figure 2.10 Typical construction process of aggregate pier: (a) Creating cavity, (b) Making the bottom bulb, (c) Building shaft with undulating layers, (d) Installation complete (Gaul, 2001)



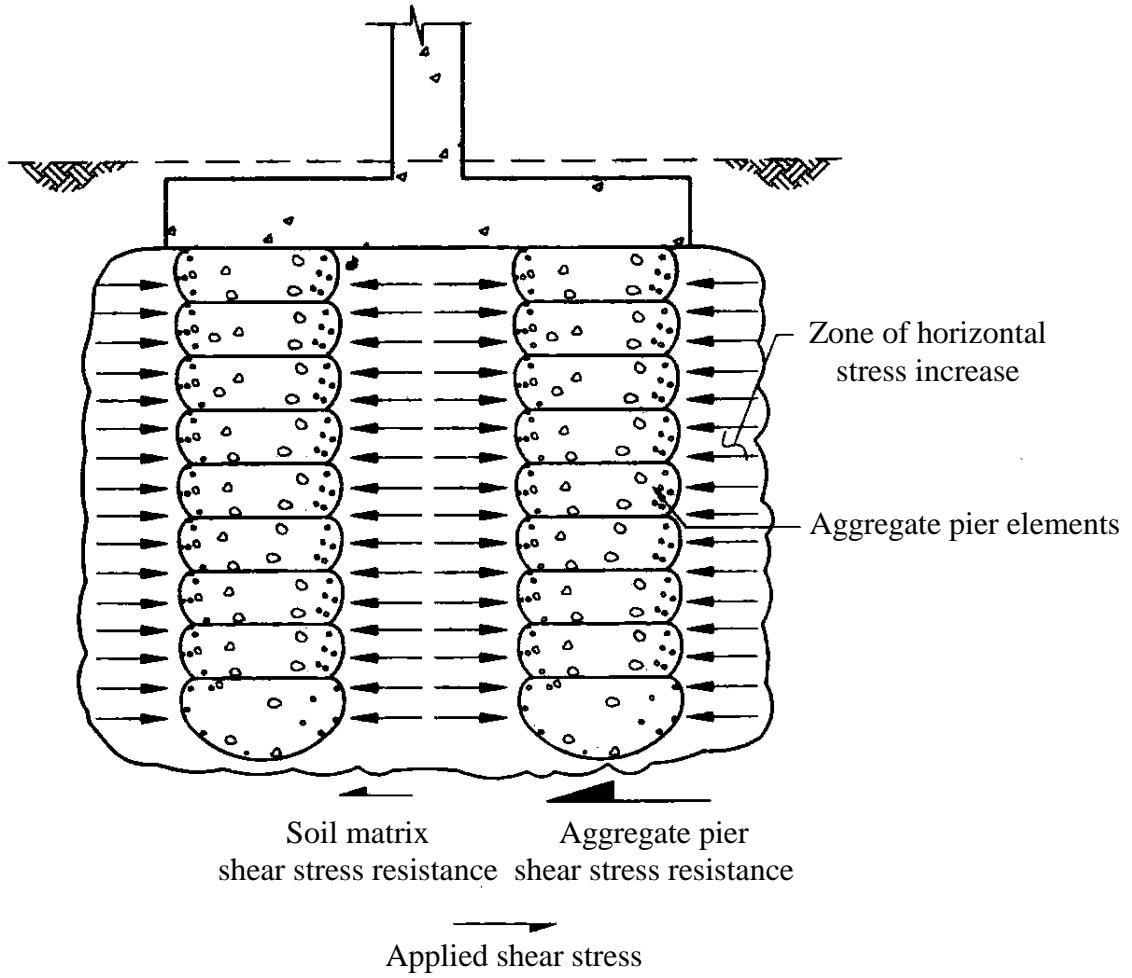


Figure 2.11 The use aggregate pier to reduce liquefaction potential (Wissmann, et al., 1999)

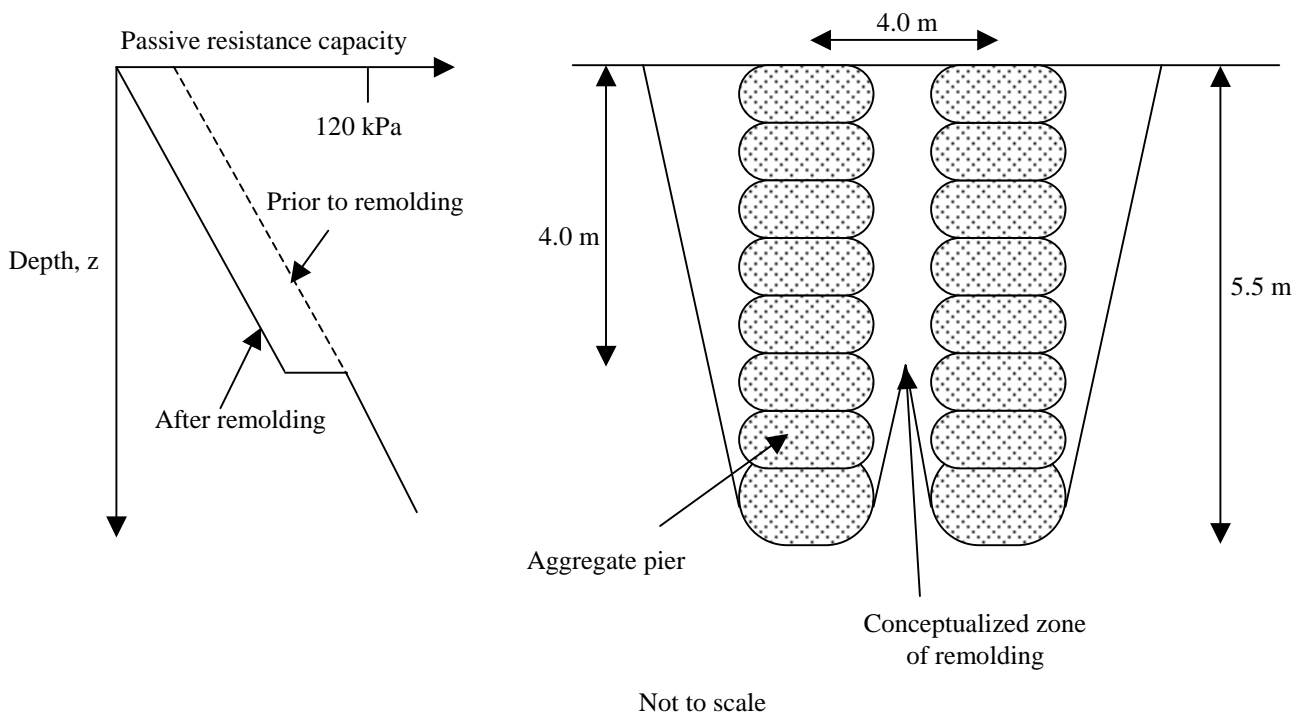


Figure 2.12 Illustration of zone of remolding (after White, et al., 2000)

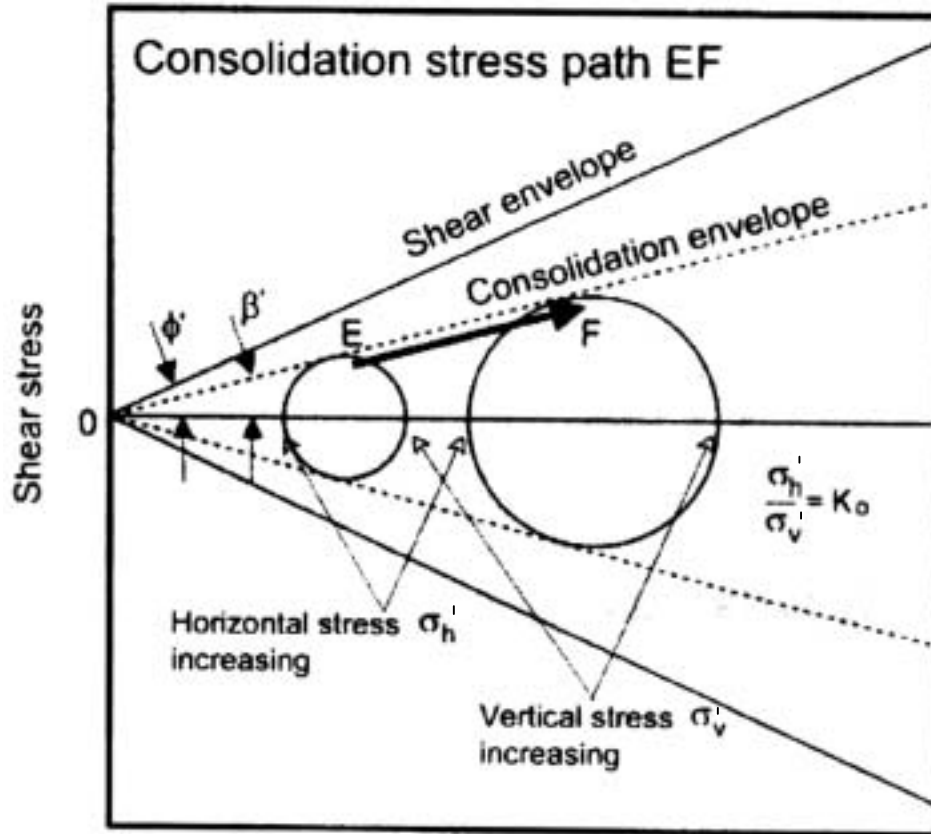


Figure 2.13 Mohr circle sequence and stress path EF during normal consolidation (Handy, 2001)

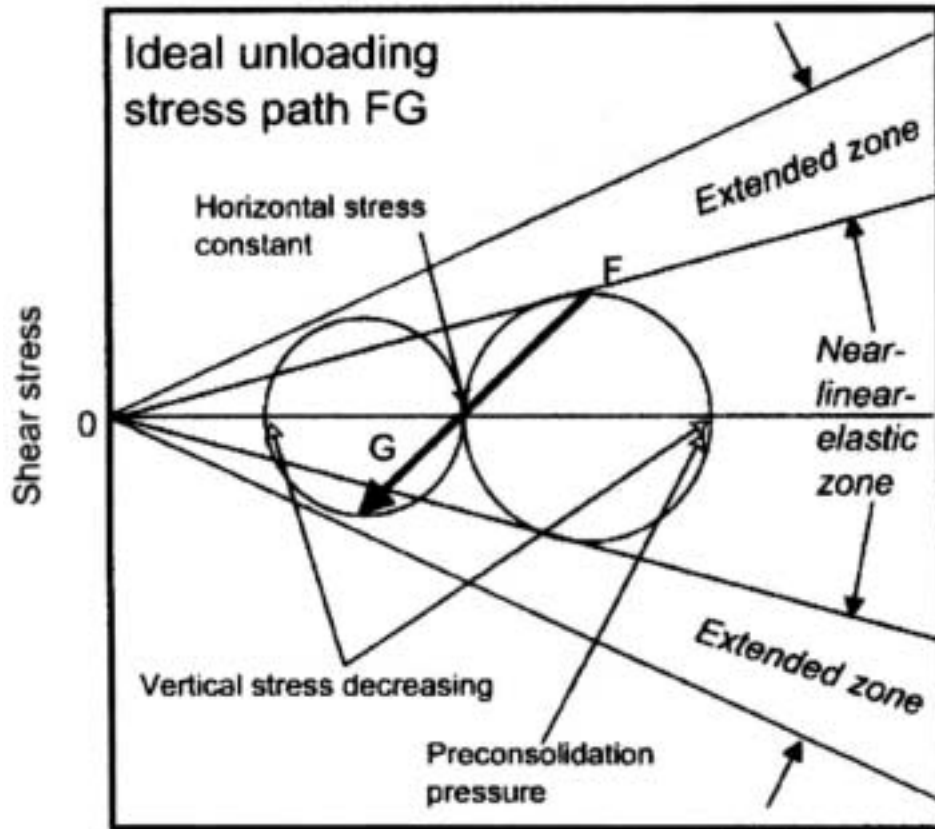


Figure 2.14 Mohr circle sequence and stress path FG as reductions in vertical stress create overconsolidated soil (Handy, 2001)

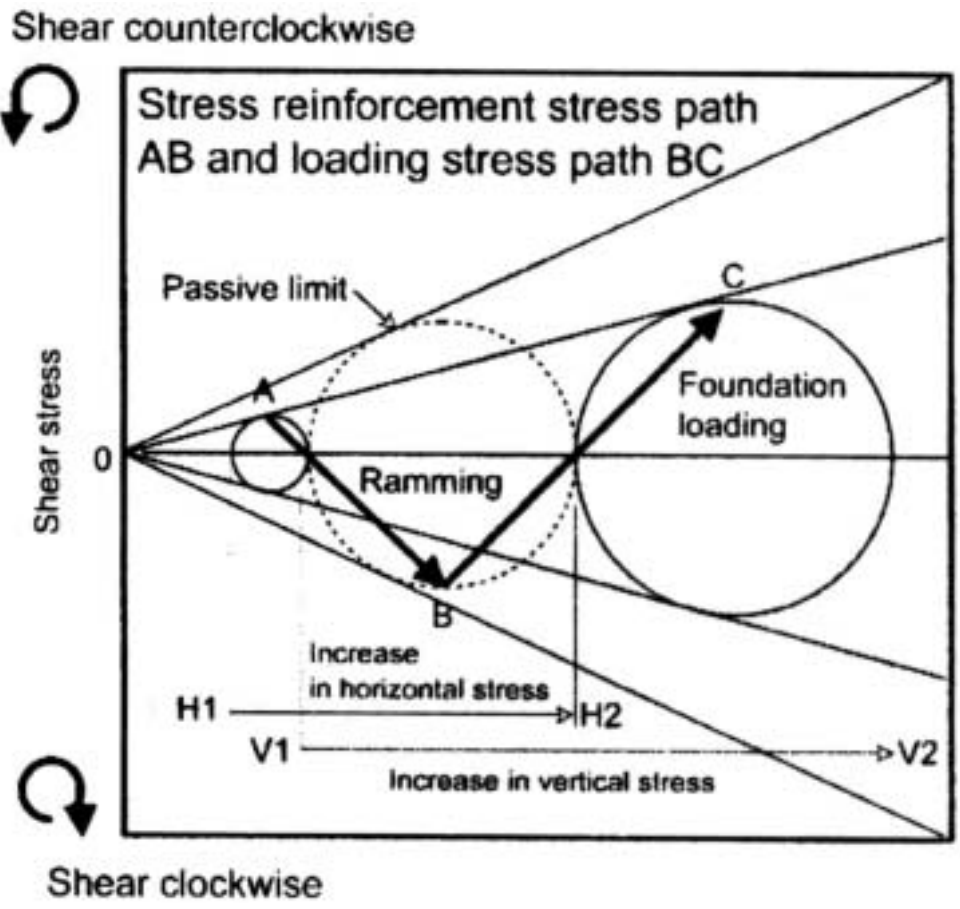


Figure 2.15 Increasing horizontal stress on normally consolidated soil (A-B) increases consolidation threshold stress from  $V_1$  to  $V_2$  (B-C) (Handy, 2001)

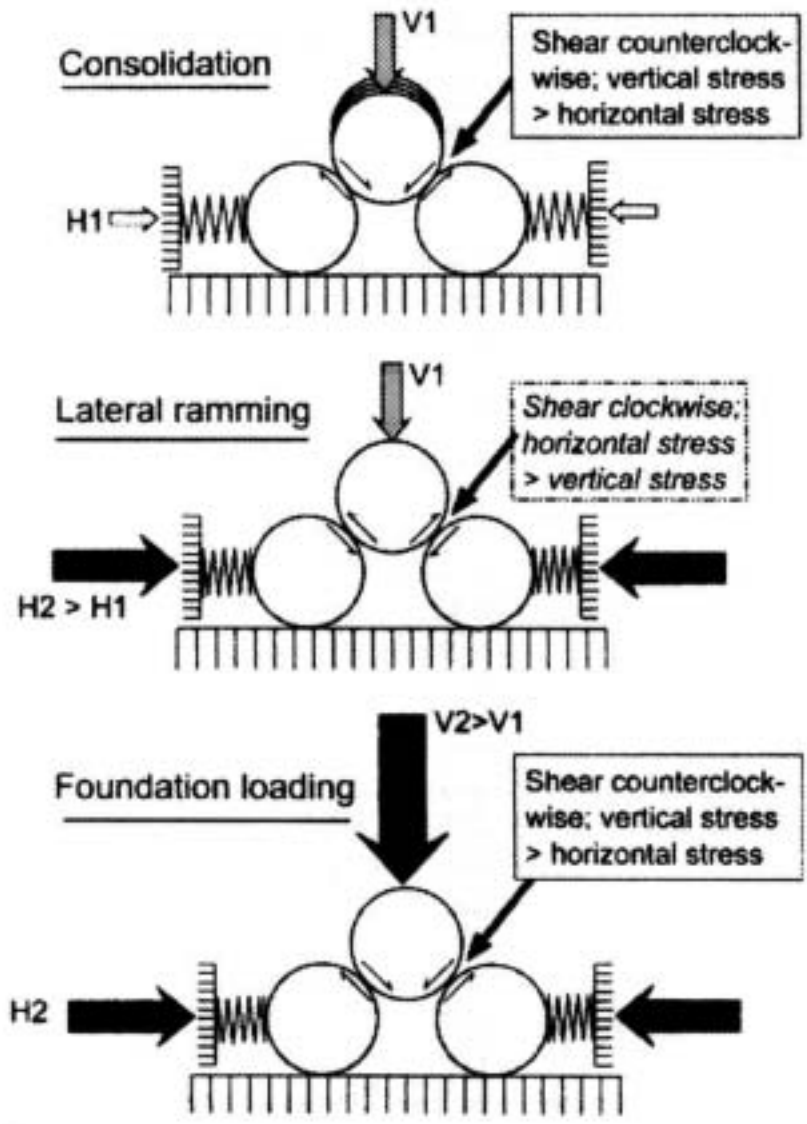


Figure 2.16 Friction reversals to explain increased vertical effective stress required to initiate consolidation in stress-reinforced soil,  $V_2$  (Handy, 2001)

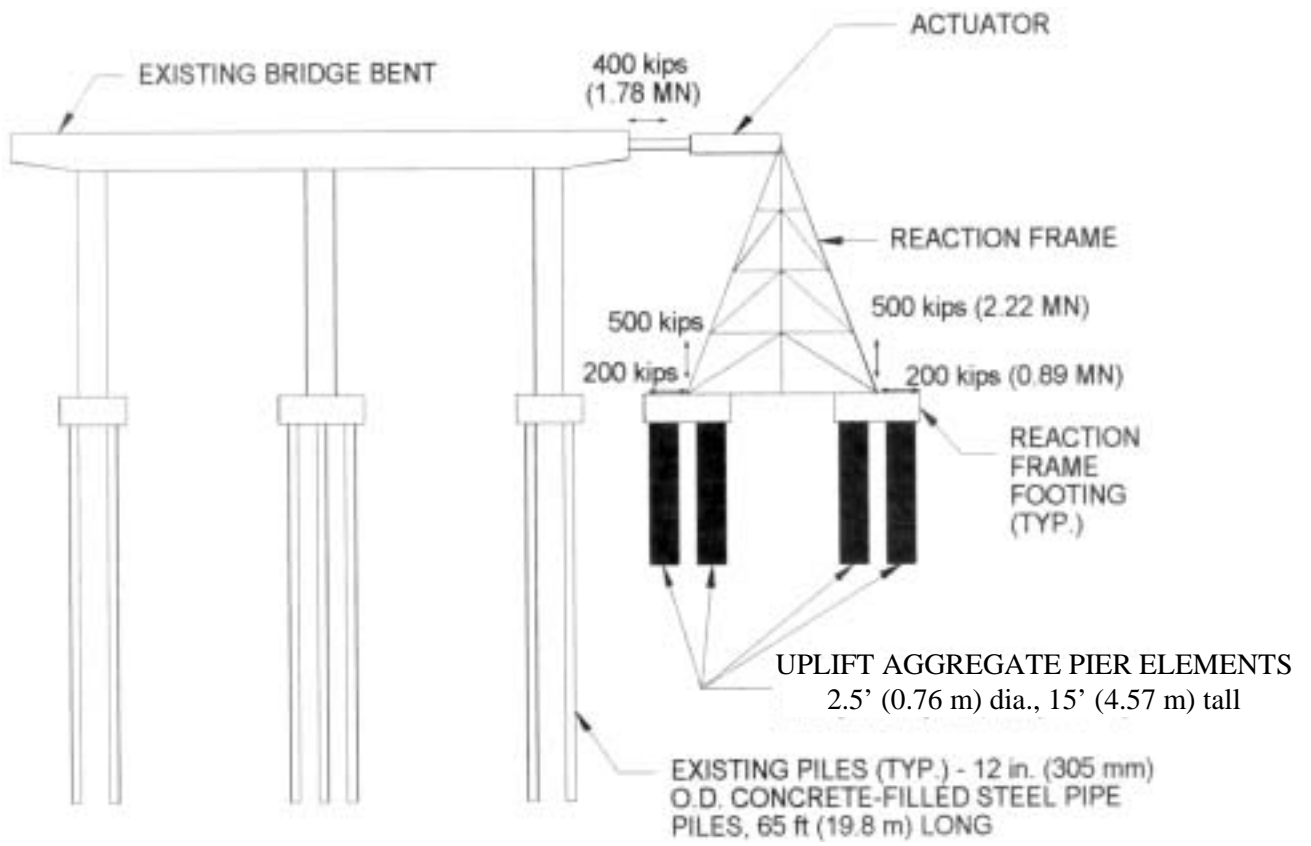
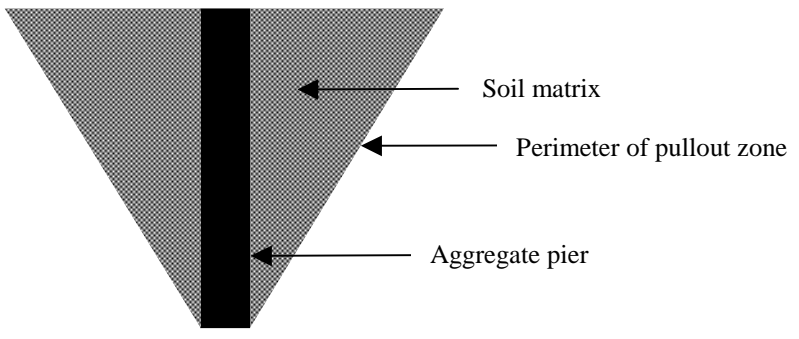
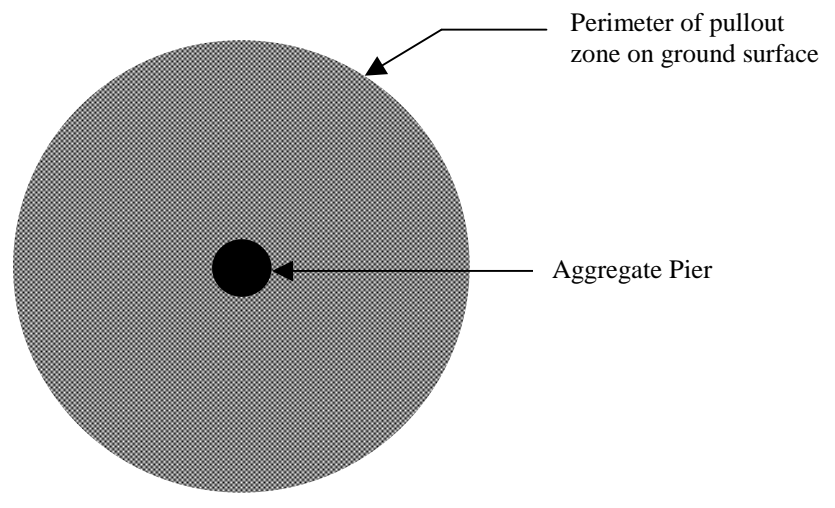


Figure 2.17 Full-scale cyclic loading test performed on aggregate piers (Lawton and Merry, 2000)



Vertical cross section



Plan view

Figure 2.18 Illustration of assumed pullout zone (after Lawton, 1999)